New Results from the SMA

James M. Moran

Harvard-Smithsonian Center for Astrophysics,
60 Garden St., Cambridge, MA 02138 USA

Abstract. The Submillimeter Array (SMA) is nearing completion in "millimeter" valley just below the summit of Mauna Kea in Hawaii. Numerous astronomical observations have been undertaken in the partially transparent bands between 0.45 and 1.3 mm. The status of the instrument is described in this paper, and examples of images that have been made with the partially completed Array of the dust and gas envelopes of a high mass protostellar object (IRAS 18089–1732), a low mass young star (LkCa15), and three evolved stars (CRL 2688, V Hydrae, and IRC+10216) are presented.

1. Introduction

The idea of an instrument to make high resolution images at submillimeter wavelengths was part of the initiative of Irwin Shapiro in 1983 as the newly appointed Director of the Center for Astrophysics, to work towards high resolution imaging capability across a broad range of the electromagnetic spectrum. At that time, arrays were in operation at Owens Valley Radio Observatory (OVRO), Berkeley Illinois Maryland Association (BIMA), Institut de Radioastronomie Millimétrique (IRAM), and Nobeyama Radio Observatory (NRO) in the three millimeter wavelength band. Exploratory observations at lower resolution with single aperture telescopes had been made at submillimeter wavelengths, especially with bolometric detectors. The challenge for high resolution submillimeter wavelength imaging was to place an instrument at a sufficiently dry site to allow operation in the partially transparent submillimeter bands and to develop sensitive receivers. The technical viability and expected scientific impact was studied at SAO and a report was written (Moran et al. 1984). Start up funding for a receiver development lab was received in 1989. The Major Instrumentation Program at SAO, initiated in 1992, was used to fund the design and construction of the Submillimeter Array (SMA) as well as to upgrade the MMT facility in Arizona. In 1996, the Institute of Astronomy and Astrophysics of the Academia Sinica of Taiwan (ASIAA) joined the SMA project and provided an additional two antennas to the initial complement of six.

2. Technical Capabilities

At this time (October 2003), the SMA is nearing completion (see Figure 1) and a number of scientific programs have already been undertaken with the partially

completed Array. Table 1 summarizes the basic characteristics of the Array. Table 2 gives the sensitivity of the instrument as a function of frequency and resolution for typical weather conditions. The collecting area of the Array is relatively modest so that the continuum sensitivity is only about 1 mJy in eight hours at 0.87 mm. However, because of the frequency squared dependence of the Rayleigh-Jeans part of the blackbody spectrum the brightness temperature sensitivity is very good compared to instruments operating at lower frequencies (i.e. the brightness temperature noise level scales as ν^2 and as θ_f^{-2} where ν is the frequency and θ_f is the angular resolution).

Figure 1.   The SMA on October 1, 2003. The eight antennas of the Array are in a hybrid configuration of the two innermost rings. At the far right is the vehicle used to transport the antennas among the 24 pads. The antennas were assembled in the building on the left with the large door. At the far left is the J.C. Maxwell telescope which, with the Caltech Submillimeter Observatory telescope (out of view on the left), will operate as part of the Array beginning in 2005. Pu'u Poli'ahu is immediately behind the Array and Mauna Loa is in the distance behind the SMA assembly building. (Photo by J. Weintroub)

The accurate alignment of the reflector surfaces is a prime achievement of the Array. One of the antennas has been successfully set to the design specification of 12 μm (See Figure 2). The SMA antennas have the most precise surfaces of any radio astronomical antennas in their size class.

An important characteristic of the instrument will be its ability to make observations at two frequencies simultaneously. This provides a convenient way to obtain polarization measurements, increased sensitivity, and correction of the phase of the higher frequency visibility measurements. Figure 3 shows the first result of two frequency operation.

Table 1. SMA Characteristics and Status in October 2003

Antennas	8 x 6–m diameter machined aluminum panels; Carbon fiber backup structures; 12 μm rms surface accuracy (current accuracies 12–27 μm)
Configuration	24 pads in 4 rings (9 pads tested)
Baselines	8–508 m (maximum tested: 120 m)
Receivers	Maximum of 8 per cryostat (2 bands simultaneously) Bands: 177–256 GHz (8 available) 256–360 GHz (8 available) 320–420 GHz (2004) 400–520 GHz (2006) 600–720 GHz (6 available) 780–920 GHz (2007)
Correlator	Hybrid analog – digital design: analog filtering to 104 MHz, effective digital sampling, with time multiplexing rate 208 MHz, 2 GHz total bandwidth. Standard mode: 2 GHz bandwidth, 0.8 MHz channel spacing, 28 baselines, two bands Higher resolution available at reduced bandwidth.
Data rate	Maximum 10 Gbyte/day Current operation: 1 receiver, 1 GHz bandwidth, 6 antennas, (i.e., 12 percent capacity)

3. Scientific Results

The problems that can be studied at submillimeter wavelengths are described in reviews by Sargent and Welch (1993), and Shaver (1996), and others. In particular, the high frequency or short wavelength end of the radio spectrum is very sensitive to thermal emission from cool dust and optically thin emission from spectral lines. Since the emissivity of dust grains varies as ν^{1-2}, the flux density from dust in the Rayleigh-Jeans regime will vary as ν^{3-4}. This means that the envelopes of many dust enshrouded star forming regions that are invisible at longer wavelengths and optically thick at optical wavelengths will be partially transparent in the submillimeter regime and readily detectable without obscuring completely the embedded sources. For optically thin spectral lines, the flux density increases as ν^4 because the Einstein A coefficient for electric

Table 2.   SMA Sensitivity

ν/λ [b] (GHz/mm)	T_{sys} [c] (K)	θ_f [d] (″)	θ_r [e] (″)	ΔT [f] (K)	ΔS [g] (mJy)
230/1.3	150	54	5.9	0.02	0.4
			0.4	5	
345/0.87	340	36	3.9	0.04	1.0
			0.25	10	
460/0.65	1870	27	2.9	0.20	5.7
			0.18	49	
690/0.43	2640	18	2.0	.024	8.7
			0.12	62	
805/0.37	4870	15	1.7	0.44	17.0
			0.10	110	

[a] Adapted from Moran (1998). Noise levels are 1σ values, based on an integration time of 8 hours.
[b] Band frequency/wavelengths are denoted by the transitions of the CO line they contain.
[c] SSB system temperatures with 1 mm of precipitable water and 1.5 air masses (opacities of 0.075, 0.26, 1.2, 1.2, and 1.2 for 230, 345, 460, 690, and 805 GHz). The (DSB) receiver temperatures are 30, 50, 70, 180, and 500 K respectively. System temperatures include a room temperature loss of 5 percent in coupling to the antenna.
[d] Field of view.
[e] Resolution for 32 m (smallest) and 508 m (largest) configurations.
[f] The Rayleigh-Jeans equivalent rms noise level in brightness temperature with 1 km s^{-1} resolution.
[g] Flux density rms noise level for a 2 GHz bandwidth.

dipole transitions scales as ν^3 and the Boltzmann factor for lines in the rotational ladder of a molecule scales as ν. Hence, a plethora of molecules can be studied in the submillimeter band (see Figure 8). For these reasons, astronomical targets such as terrestrial planetary bodies, gas in molecular clouds in the Milky Way and external galaxies, and high redshift "SCUBA" galaxies can be readily studied. In addition, the flux density from very compact optically thick synchrotron sources varies as $\nu^{2-2.5}$. Many interesting objects, such as the radio source Sgr A*, are particularly prominent at submillimeter wavelengths (Zhao et al. 2002).

In keeping with the scientific focus of this conference, I have concentrated the discussion of early SMA observations on those related to stars. The SMA does not have the sensitivity to detect black body photospheric emission from any but the closest main sequence stars. Its application is primarily to stars with extended envelopes, including newly formed stars and evolved stars. Several examples of early observations are described below.
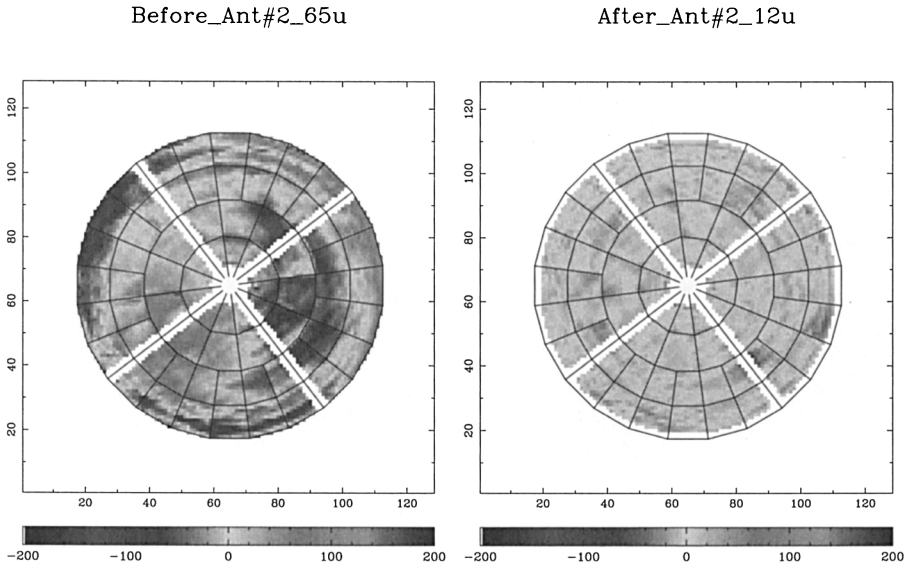
Before_Ant#2_65u   After_Ant#2_12u

Figure 2. The reflector of each antenna has 72 machined aluminum panels with rms surface accuracies of 5 μm or smaller. The figure of each of the reflectors was accurately determined by the technique of radiometric holography by use of a 230 GHz beacon mounted on the pier of the Subaru telescope. The figure of a reflector after its initial mechanical adjustment to an accuracy of 65 μm, is shown on the left. Its figure after the final adjustment to 12 μm accuracy is shown on the right. (From T.K. Sridharan, private communication)

3.1. The EGG Nebula (CRL 2688)

The Egg nebula is a protoplanetary nebula that evolved from an AGB star about 10^2 years ago. The image of the CO emission in the Egg Nebula was among the first images made with the SMA when it began operation in 2001 at 345 GHz with four antennas. The image of the CO(3-2) emission is shown in Figure 4, along with the optical image from the HST. The CO image shows the bipolar outflow in the direction of the optical extension and also a secondary orthogonal flow. The morphology is very similar to that reported for the CO(2-1) emission imaged with the IRAM Array (Cox et al. 2000).

3.2. V Hydrae

V Hydrae is a carbon star located at a distance of 380 pc, which is on the AGB part of the HR diagram or has recently evolved into a post AGB stage. It has a mass loss rate of about 10^{-6} solar masses per year. Low resolution observations have shown an asymmetrical envelope with high velocity emission (e.g., Knapp, Jorissen, and Young 1997). The SMA provided the first images of the CO(3–2) and CO(2–1) emission at 345 GHz and 230 GHz (Hirano et al. 2003) from this

star. Data were obtained on a total of 15 baselines, which provided a resolution of four arcseconds (1500 AU). The emission shows an extended structure in the NS direction with a velocity flow of $\pm$ 40 km s^{-1} and size of 20 x 12 arcseconds (7600 x 4600 AU), as well as bipolar jets in the EW direction with velocities of $\pm$ 150 km s^{-1}. Figure 5 shows the data and a simplified model of the star's circumstellar structure.

3.3.   IRC10216

IRC10216 is an evolved star with an extended carbon rich envelope. Its chemistry has been extensively studied with millimeter wavelength interferometers. This star was the first source imaged by the SMA in the 690 GHz band. At the time of the observations in December 2002, the Array had only three antennas in operation at 690 GHz. Phase calibration of the Array presents a major problem in this frequency band. By fortunate circumstance, Callisto, a moon of Jupiter, was only seven degrees away and served as a bright phase calibrator source of 57 Jy. The envelope is an approximately spherically symmetric outflow within which the molecular constituency changes as a function of radius. The emission from CS(14–13), imaged as a function of velocity (Young et al. 2003) and shown in Figure 6, arises close to the stellar photosphere. As with other molecular emission, the most compact emission is at the highest and lowest velocities, which arises from the caps of the shell in front of and behind the star, while the emission at the velocity of the star arises from the tangentially outflowing gas.
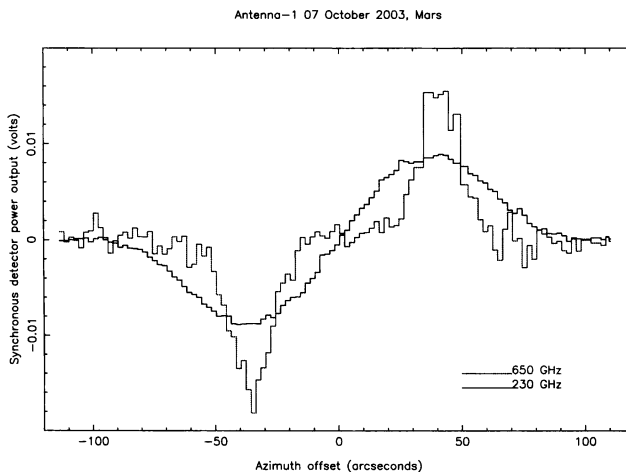

Figure 3.   Scans of Mars made simultaneously at the frequencies 230 and 690 GHz, with the chopping secondary, which has a throw of 80 arcseconds, running. The optics are aligned to an accuracy of about 10 arcseconds. (From N. Patel, private communication)
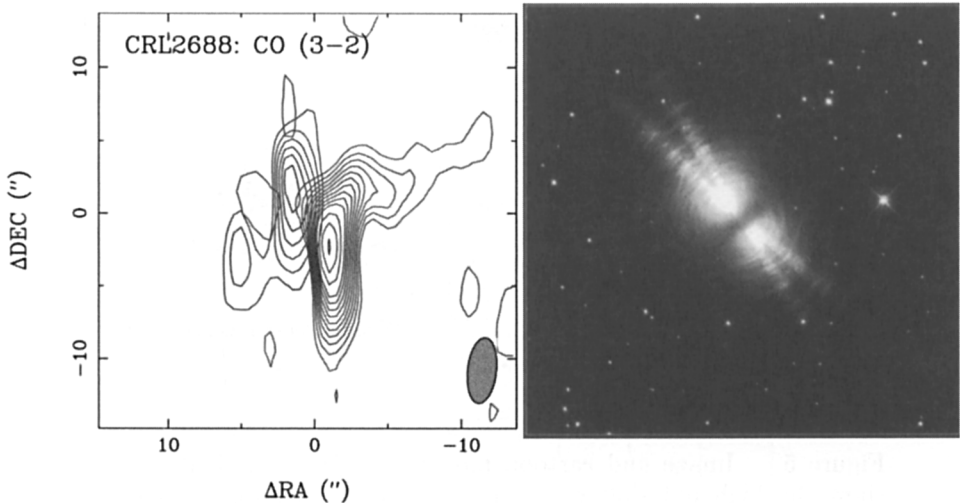
Figure 4.   Right: an optical image of the Egg Nebula (CRL2688) made with the Hubble Space Telescope which shows a bipolar structure. Left: image made of the high velocity components of the CO(3–2) transition (dark and light contours), which shows an additional outflow along a SE–NW axis. (From N. Patel, private communication)

3.4.   LkCa 15

LkCa 15, a K5 star located in the Taurus-Auriga molecular cloud complex at a distance of 140 pc, is one of the best studied T Tauri stars at millimeter wavelengths. Its age has been estimated to be between 3 and 12 $\times 10^6$ years. Previous interferometric observations in the CO(2-1) transition by Duvert et al. (2000) and Qi et al. (2003) show a gaseous disk extending out to about 700 AU with a velocity gradient that is a clear indication of Keplerian rotation. The disk ellipticity suggests that its inclination angle is about 60°. The image of the CO(3-2) emission made with the SMA with a resolution of about 4″ shows the previously identified rotational signature and the distribution of the hotter gas (see Figure 7).

3.5.   IRAS 18089–1732

IRAS 18089–1732 is a very young high mass object, which is either a protostar or a newly formed star (Sridharan et al. 2002). Its distance is 3.6 kpc and it has a bolometric luminosity of $10^{4.5}$ solar luminosities. Images and spectra obtained with the SMA are shown in Figure 8 (Beuther 2003).

The high spectral resolution and wide spectral bandwidth of the SMA spectrometer shows a rich molecular envelope in this object. All of the spectral lines can be imaged simultaneously and selected examples are shown in the figure.
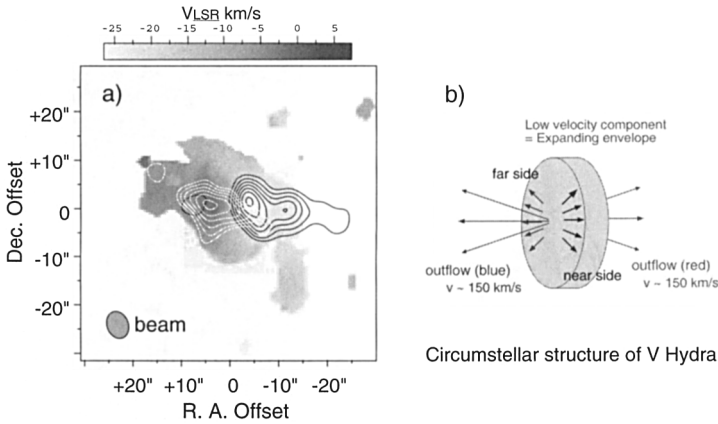
Figure 5.   Image and cartoon model of V Hydrae. Left: contours show the high red–shifted (solid line) and blue–shifted (dotted line) emission in the CO(2–1) transition. The distribution of the mean velocity of the gas is shown in the shaded image. Right: model of the stellar envelope showing a low velocity expanding disk and a high velocity polar outflow ($\pm$ 150 km s^{-1}.) (From Hirano et al. 2003)

The HCN and SO emission, which is displaced from the core (thermal dust continuum emission) traces parts of the molecular outflow.

4.   Instrument Development and Use

By the end of 2004, we expect that the SMA will operate smoothly with all eight antennas in the 230, 345, or 690 GHz bands with full bandwidth of 2 GHz. There are three major projects for 2004.

The first project will be to double the data rate by allowing operation in two bands simultaneously. This goal will require doubling the IF processing capability and the correlator capacity. The equipment is in hand and the task is one of system integration. In addition to doubling the data acquisition rate, the dual frequency operation will enable a calibration strategy of using the 230 GHz band as a phase reference for the higher band where calibration sources are weaker and the phase fluctuations caused by the atmosphere are larger. The second major project will be to build receivers for the 320–420 GHz band (see Table 2). The 40 GHz overlap with the 256–360 GHz will be particularly useful. It will improve the sensitivity in a fixed integration time for observations of sources in the overlap band. Since the receivers will have orthogonal linear polarizations, complete and efficient determination of the polarization parameters of sources will be possible without the use of time–multiplexed quarterwave plates. The third project will be the integration of the JCMT and CSO telescopes into the array for observations in the 345 GHz band. The correlator has the capacity to
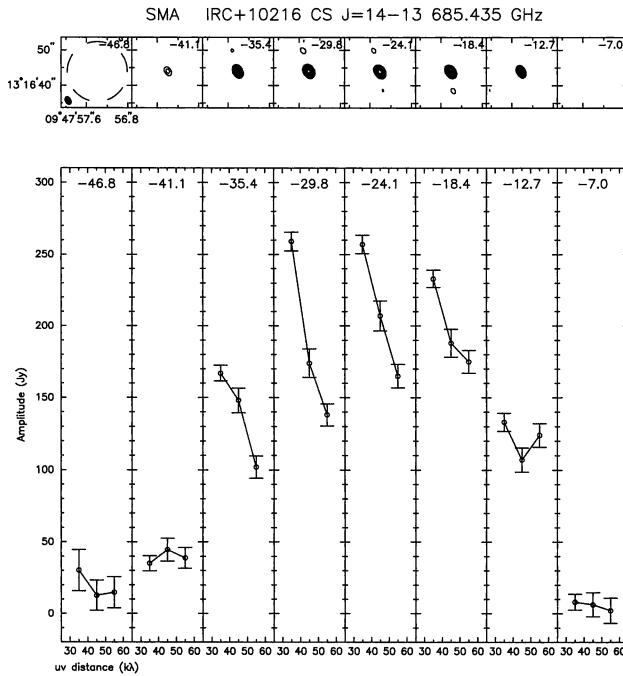
Figure 6. Top: images of IRC+10216 in the CS(14–13) transition at 685 GHz as a function of velocity from –46.8 to –7.0 km s^{-1}. The leftmost panel shows the field of view imaged and the resolution beam. Bottom: fringe visibility amplitude as a function of baseline length for various velocities. Rapidly declining visibility functions indicate large component sizes. (From Young et al. 2003)
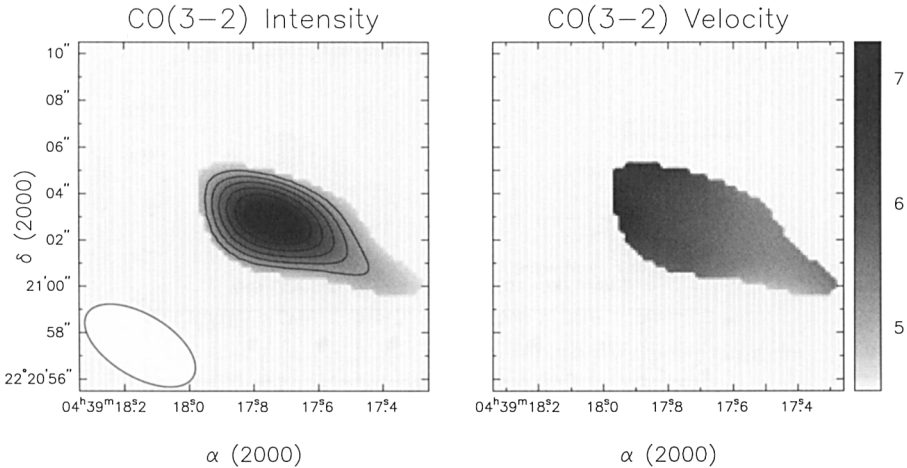
Figure 7.   LkCa15. Left: Image in the CO(3–2) transition, with
the beam shown in lower left. Right: average velocity distribution
which shows a gradient indicative of rotation. (From C. Qi, private
communication)

process data for 10 antennas on 45 baselines. The combined array will improve
the u–v plane coverage of the Array, increase the resolution by 50 percent, and it
will more than double its collecting area. An agreement has been reached among
the observatories to dedicate specific periods of 2005 for 10 station operation on
projects selected by a special telescope Time Allocation Committee.

Starting in 2005, receivers for the bands 400–520 GHz and 780–920 GHz
will be installed. In the higher band, the technology for providing sensitive SIS
receivers and reliable local oscillator power sources is rapidly improving.

There is room on Mauna Kea to conveniently extend the baselines with
outlying stations, which would allow for the doubling of the resolution. Such a
plan is contained part of the Mauna Kea Science Reserve Master Plan (University
of Hawaii, 2000). However, any such expansion would require a complete review
by relevant oversight authorities.

More information about the SMA can be found on the project website
(http://sma-www.cfa.harvard.edu). A restricted website, which provides daily
updates of the Array status and observational results, is also maintained for
interested parties (contact rcarey@cfa.harvard.edu for access).
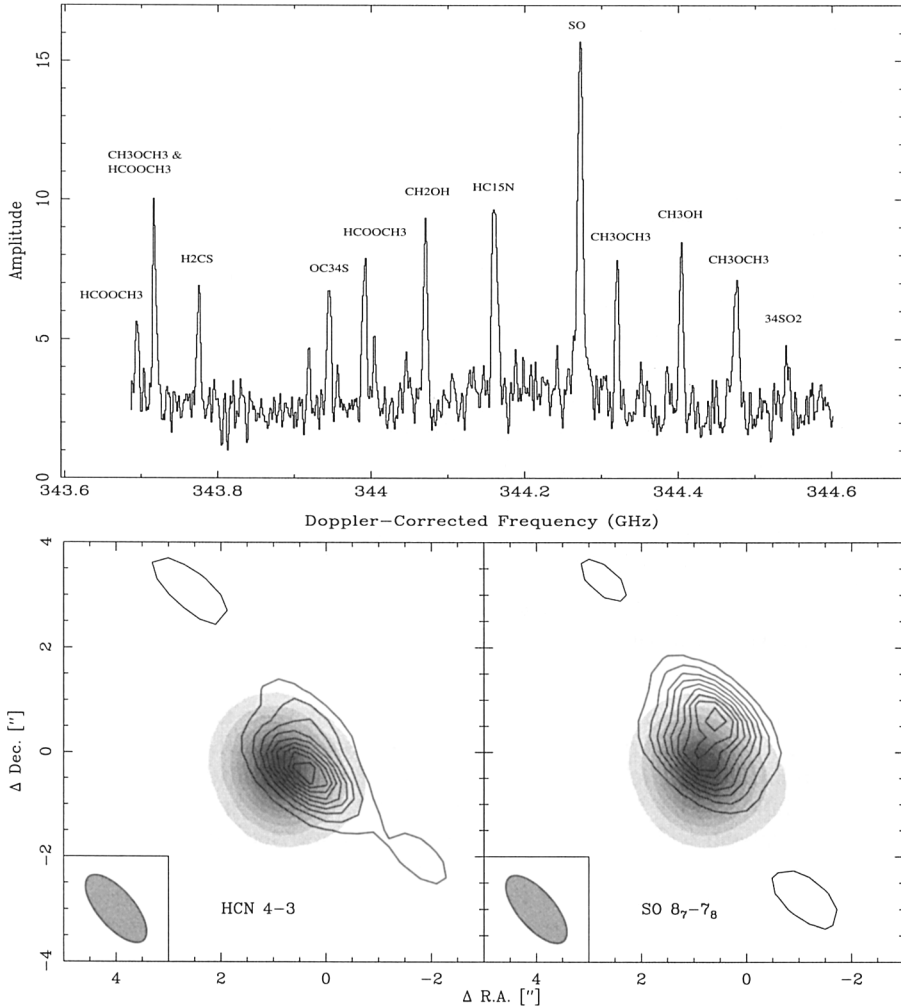
Figure 8.   IRAS 18089–1732. Top: spectrum in a 1 GHz spectrometer window around 344 GHz, which shows many molecular transitions. Lower left: intensity contours of the HCN(4–3) emission superimposed on the continuum emission (dust continuum) shown in gray scale. Lower right: intensity contours of SO($8_8 - 7_7$) emission. (From Beuther 2003)

References

Beuther, H. 2003, ASP 221, in Star Formation at High Angular Resolution, ed. R. Jayawardhana, M.G., Burton, & T.L. Bourke (San Francisco: ASP)

Cox, P., Lucas, R., Huggins, P.J., Forveille, Bachiller, R., Guilloteau, S., Maillard, J.P., & Omont, A. 2000, A&A, 353, L25

Duvert G., Guilloteau, S., Menard, F., & Dutrey, A. 2000, A&A 355, 165

Hirano, N. et al. 2003, in Asymmetric Planetary Nebulae III, ASP Conference Series, ed. M. Meixner, J. Kastner, B. Balick, N. Soker, (San Francisco: ASP) in press

Knapp, G.R., Jorissen, A., & Young, K. 1997, A&A 326, 318

Moran, J.M. 1998, Proc. SPIE, 3357, 208

Moran, J.M., Elvis, M.S., Fazio, G.G., Ho, P.T.P., Myers, P.C., Reid, M.J., & Willner, S.P. 1984, SAO internal report

Qi, C., Kessler, J.E., Koerner, D.W., Sargent, A.I., & Blake, G.A. 2003 ApJ, 597, 986

Sargent, A.I. & Welch, W.J. 1993, ARAA, 31, 297

Shaver, P.A. 1996, Science with Large Millimeter Arrays, (Springer: Berlin)

Sridharan, T.K., Beuther, H., Schilke, P., Menten, K.M., & Wyrowski, F. 2002, ApJ, 566, 931

University of Hawaii, Mauna Kea Science Reserve Master Plan 2000

Young, K.H. et al. 2003, in preparation

Zhao, J.–H., Young, K.H., Herrnstein, J.R., Ho, P.T.P., Tsutsumi, T., Lo, K.Y., Goss, W.M., & Bower, G.C. 2003, ApJ, 586, L29